The Effect of Current on Skin Barrier Function *In Vivo*: Recovery Kinetics Post-Iontophoresis

Norris G. Turner,[1,2] Yogeshvar N. Kalia,[1,3,4] and Richard H. Guy[1,3,4,5]

Received January 19, 1997; accepted June 4, 1997

Purpose. The objective of this study was to determine the extent to which current passage perturbed the skin's intrinsic permeability, and to quantify how quickly and to what extent the barrier properties recovered from the effects of iontophoresis.

Methods. Laser scanning confocal microscopy (LSCM) and impedance spectroscopy (IS) were employed, respectively, to visualize and quantify the recovery kinetics.

Results. LSCM images were obtained following *passive* calcein diffusion through pre-iontophoresed HMS skin *in vivo* that had been allowed to recover for progressively longer periods of time. IS was used to quantify the rate and extent of skin permeability recovery following current pretreatment. Impedance spectra were recorded 0, 3, 5, 7, 9 and 18 hrs after current termination.

Conclusions. Enhanced calcein permeability as assessed by confocal microscopy persisted for up to 24 hrs following current passage. Consistent with these LSCM findings, IS indicated that the time required for the impedance of hairless mouse skin to return to pre-iontophoresis levels (following 2-hr current passage at 0.5 mA/cm^2) was at least 18 hrs.

KEY WORDS: iontophoresis; skin; barrier function; recovery kinetics; transport; impedance spectroscopy.

INTRODUCTION

The relative impermeability of the skin to ion transport may be attributed almost entirely to the effective barrier function of the outermost, and least permeable skin layer, the stratum corneum (SC). Constant-current iontophoresis is able to enhance the transdermal flux of a broad range of ionizable molecules, including therapeutic peptides and proteins. However, to achieve this objective, some compromise in skin barrier function is anticipated. Understanding the effects of current on the skin is critical, therefore, to establish the therapeutic feasibility of iontophoresis (1). At present, though, evidence is limited regarding (a) the mechanism(s) by which the barrier properties of skin are impaired during current passage, and (b) the kinetics and extent *in vivo* of the subsequent recovery following iontophoresis.

In vitro experiments have shown that the skin's ability to recover from current-induced effects is impaired (2–9). However, under these conditions, the skin lacks circulation and is metabolically compromised. To circumvent this limitation, we designed an experimental approach to examine the effect of iontophoresis on hairless mouse skin (HMS) *in vivo*. Laser scanning confocal microscopy (LSCM) permitted the recovery and re-establishment of pretreatment-level barrier function to be visualized directly. Relaxation of skin permeability was also quantified by impedance spectroscopy (IS) which is able to characterize noninvasively the electrical properties of the barrier. Skin impedance measures the difficulty encountered by ions as they move through the membrane: if skin barrier function is compromised, then ion transport is easier and the impedance decreases. Skin impedance also decreases with increasing tissue hydration (10,11), which facilitates ion uptake into the skin. IS has been used previously to evaluate the effect of current on skin impedance (10,12–14), the ability of the skin to recover following current passage (6,10,12,15), and the development of equivalent circuit models to explain the mechanism of iontophoresis (10).

Thus, our major objective was to determine the extent to which current passage perturbed the skin's intrinsic permeability, and to quantify how quickly and to what extent the barrier properties recovered from the effects of iontophoresis. It was also our intent to measure how different putative transport pathways (i.e., follicular, intercellular) were affected and to assess their ability to recover from the electrical perturbation.

MATERIALS AND METHODS

Chemicals

Chromatographically-purified calcein (MW 623), a polyanionic fluorescent probe, was used as the model permeant in LSCM experiments (Molecular Probes, Eugene, Oregon). Deionized water (resistivity $\geq$ 18 MΩ cm^{-1}) from a Milli-Q UF Plus purification system (Millipore Corp., Bedford, MA), was used to prepare all aqueous solutions.

Experimental Apparatus

Glass diffusion chambers (diameter = 1 cm) [LGA, Berkeley, California] and silver/silver chloride reversible electrodes were used in all *in vivo* iontophoresis experiments. Constant current was supplied from a custom-built power supply (Professional Design and Development Services, Berkeley, California) interfaced to a MacIntosh IIfx computer (Apple Computer Inc., Cupertino, California) running LabView 2.1.1 software (National Instruments Inc., Austin, TX).

Recovery of Passive Permeability Measured by Confocal Microscopy

Iontophoresis

HRS/hr female hairless mice (HMS), 8 to 12 weeks old, were anesthetized for approximately 3.5 hrs by intraperitoneal

[1] Departments of Biopharmaceutical Sciences and Pharmaceutical Chemistry, University of California—San Francisco, San Francisco, California 94143-0446.

[2] Current address: Department of Molecular Pharmacology, Stanford University Medical Center, Stanford, California 94305-5332.

[3] Centre Interuniversitaire de Recherche et d'Enseignement, "Pharmapeptides", Campus Universitaire, Parc d'Affaires International, F-74166 Archamps, France.

[4] Université de Genève, Section de Pharmacie, 30 quai E. Ansermet, CH-1211 Genève 4, Switzerland.

[5] To whom correspondence should be addressed. (e-mail: rhg@pharma1.cur-archamps.fr)

0724-8741/97/0900-1252$12.50/0

injection of 0.2 mL of 40 mg/mL chloral hydrate. Diffusion chambers were adhered to the dorsal/ventral skin of the mouse with cyanoacrylate glue (Borden Inc., Columbus, Ohio). Electrolyte solution (25 mM HEPES buffer in 133 mM NaCl, adjusted to pH 7.4) was introduced, the electrodes inserted and connected to the power supply. Then, typically, constant current at 0.5 mA/cm^2 was applied for two hours. Each mouse served as its own control. Three procedures were performed (two of which were controls): (a) Treatment—Immediately following current passage, the electrolyte in the cathode chamber was removed and the skin was allowed to "recover" for 0, 1, 18, 24, or 48 hrs. Following the recovery period, the cathodal chamber was refilled with 0.05 mM calcein which was allowed to passively diffuse across the skin for one hour. Then, the mouse was sacrificed by CO_2 euthanasia, the skin which had been situated beneath the cathode was excised, and the sample was prepared for confocal visualization. (b) Control #1—Same as above, except that no current was applied. These passive controls were performed on the same mice as those which were *current-treated* in part (a). (c) Control #2—The 2-hr iontophoresis treatment was performed with 0.05 mM calcein present in the electrolyte placed in the cathodal chamber. At the end of iontophoresis, the mouse was sacrificed immediately, and the skin beneath the cathode was removed for LSCM visualization.

Confocal Microscopy—Visualization

A Bio-Rad MRC 600 Laser Scanning Confocal Microscope [Bio-Rad Microscience Ltd., Hemel Hempstead, UK] was employed for imaging. The illumination light source was a Krypton-Argon laser. The principal laser line was 488 nm. Only in-focus light is detected with this technique, enabling non-destructive optical sectioning of the tissue to be performed.

Recovery of Passive Permeability Measured by Impedance Spectroscopy (IS)

A MacIntosh Quadra 800 (Apple Computers Inc., Cupertino, California) equipped with LabView 2.1.1 software (National Instruments Inc., Austin, Texas) was used to control a pulse/function generator (HP8116A Hewlett-Packard Co., North Hollywood, California). A sinusoidal alternating current (ac), the frequency of which was increased from 1 Hz to 1.6kHz incrementally with 10 frequency points sampled per decade, was produced from an applied voltage of 1.0V (peak-to-peak). To ensure the passage of a small sinusoidal input current, a 2 MΩ resistor in series with the skin was included in the electrical circuit. Thus, at the applied voltage of 1.0V (peak-to-peak), the sinusoidal current remained approximately constant (≈0.25 μA). The potential difference across the skin was measured using a lock-in amplifier (SR850 DSP, Stanford Research Instruments Inc., Sunnyvale, California). Microsoft Excel (version 4.0, Microsoft Corp., Redmond, Washington) was used to analyze all impedance data.

Anodal and cathodal electrode chambers were firmly adhered with cyanoacrylate glue to the skin of anesthetized hairless mice. Silver/silver chloride electrodes were placed in the diffusion chambers, which were filled (~0.6 mL) with 25 mM HEPES buffer (in 133 mM NaCl at pH 7.4). Passive and hydrated impedance spectra were first recorded. These impedance measurements were made immediately after application of buffer solution to the skin (the passive measurement) and then following 10 minutes of skin hydration (the hydrated measurement). By this time, the low frequency impedance (i.e., the resistive component) had fallen to an essentially constant value. Subsequently, one of three *in vivo* iontophoretic treatment regimens were performed (n = 3 mice for each): (a) 0.10 mA/cm^2 applied for 15 minutes; (b) 0.10 mA/cm^2 applied for 2 hrs; (c) 0.50 mA/cm^2 applied for 2 hrs.

Impedance spectra were then recorded at 0, 3, 5, 7, 9 and 18 hrs after termination of current flow. As for the pre-treatment, the spectra at each time point were recorded after a 10 minute hydration period. Impedance (Z_s) data are presented as Bode plots of log [Z_s] versus log [ω] (log of the angular frequency in units of rad s^{-1}). To simplify comparisons, the absolute impedance values were normalized with respect to the pre-iontophoretic (hydrated skin) impedance measured at 1Hz (6.28 rad s^{-1}).

RESULTS

Recovery of Passive Permeability Measured by Confocal Microscopy

Figure 1 (upper panel) shows a z-series of confocal images obtained following 2 hrs of calcein iontophoresis across HMS *in vivo*. In these images (compared to those of the passive control in the lower panel), calcein transport to deeper layers in the skin (i.e., 20–40 μm) clearly involved significant participation of the follicular (F) pathway. Confocal images obtained following the *in vivo* iontophoresis of calcein served as an important control, with which to compare *passive* calcein diffusion through pre-iontophoresed skin that had then been allowed to recover for progressively longer periods of time (0, 1, 18, 24 and 48 hrs). When no time was allowed for barrier recovery ($t_{recovery}$ = 0 hrs), confocal images revealed significantly increased passive penetration of calcein along the F pathways

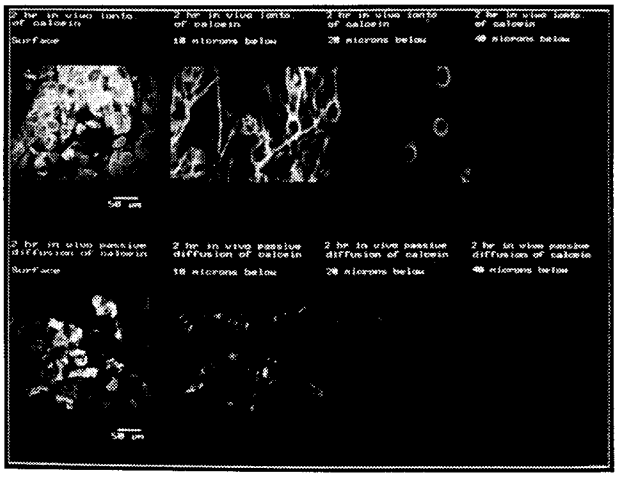

Fig. 1. LSCM images of HMS obtained 2 hrs after a) the cathodal iontophoresis of calcein (upper panel of four images), and b) the passive diffusion of calcein (lower panel of four images). The images were obtained by optical sectioning at skin depths of 0, 10, 20 and 40 μm below the skin surface (arranged from left to right). Magnification was 40× for all images.

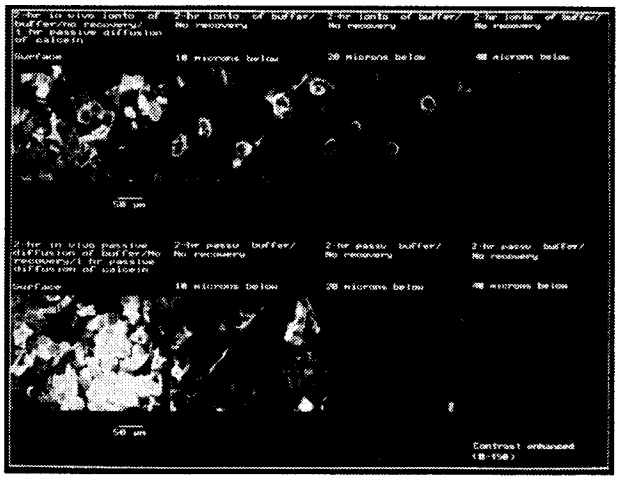

Fig. 2A. LSCM images of HMS obtained after: a) (upper panel of four images) iontophoretic pretreatment with HEPES buffered saline at pH 7.4 for two hours. There was no recovery period. Immediately after termination of the current, calcein was placed in the cathodal chamber and then allowed to passively diffuse across HMS *in vivo* for one hour. b) (lower panel of four images) Same as above except that no current was passed (control). In the upper and lower panels, images were obtained by optical sectioning at skin depths of 0, 10, 20 and 40 μm below the skin surface (arranged from left to right). Magnification was 40× for all images. The images were contrast enhanced.

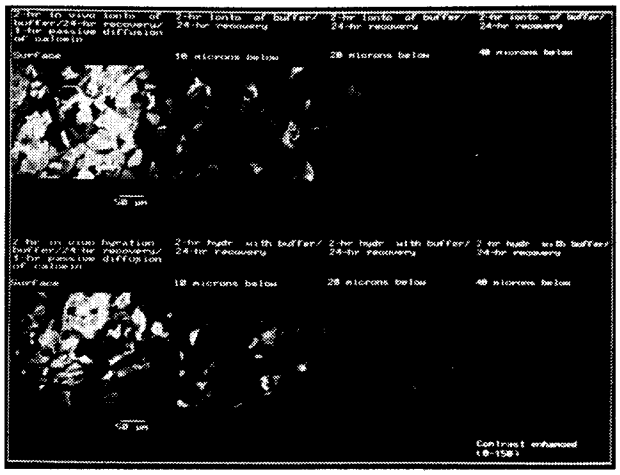

Fig. 2C. LSCM images of HMS obtained after: a) (upper panel of four images) iontophoretic pretreatment with HEPES buffered saline at pH 7.4 for two hours. There was a 24 hr recovery period. Immediately after termination of the current, calcein was placed in the cathodal chamber and then allowed to diffuse passively across HMS *in vivo* for one hour. b) (lower panel of four images) Same as above except that no current was passed (control). In the upper and lower panels, images were obtained by optical sectioning at skin depths of 0, 10, 20 and 40 μm below the skin surface (arranged from left to right). Magnification was 40× for all images. The images were contrast enhanced.

(Figure 2A, upper panel). In fact, the elevated passive permeability of calcein was comparable, in both distribution and extent (at the level of LSCM), to that achieved by the direct iontophoresis of calcein (Figure 1). With a 1 hr recovery period, the current-induced increase in the passive permeability of the skin remained obviously elevated above the control level (Figure 2B). The images recorded after 18 and 24 hours post-current passage (Figure 2C) show that there has been an appreciable recovery of the barrier, with only a few and occasional areas of increased fluorescence persisting. At 48-hrs, the current-

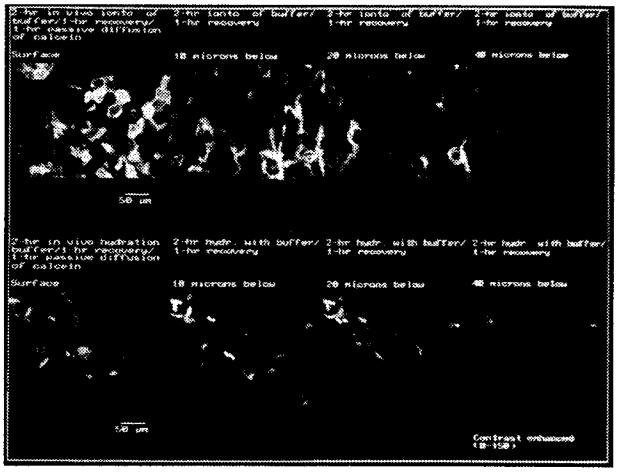

Fig. 2B. LSCM images of HMS obtained after: a) (upper panel of four images) iontophoretic pretreatment with HEPES buffered saline at pH 7.4 for two hours. There was a one-hour recovery period. Immediately after termination of the current, calcein was placed in the cathodal chamber and then allowed to diffuse passively across HMS *in vivo* for one hour. b) (lower panel of four images) Same as above except that no current was passed (control). In the upper and lower panels, images were obtained by optical sectioning at skin depths of 0, 10, 20 and 40 μm below the skin surface (arranged from left to right). Magnification was 40× for all images. The images were contrast enhanced.

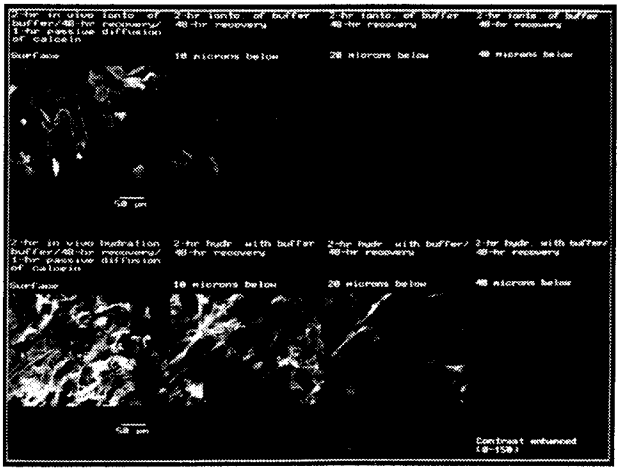

Fig. 2D. LSCM images of HMS obtained after: a) (upper panel of four images) iontophoretic pretreatment with HEPES buffered saline at pH 7.4 for two hours. There was a 48 hr recovery period. Immediately after termination of the current, calcein was placed in the cathodal chamber and then allowed to passively diffuse across HMS *in vivo* for one hour. b) (lower panel of four iamges) Same as above except that no current was passed (control). In the upper and lower panels, images were obtained by optical sectioning at skin depths of 0, 10, 20 and 40 μm below the skin surface (arranged from left to right). Magnification was 40× for all images. The images were contrast enhanced.

exposed and control confocal images were not in any way different (Figure 2D), suggesting that on the order of 24 hrs is required for the HMS barrier to recover from a 2-hr exposure to 0.5 mA/cm^2 (a current density generally considered to be the maximum tolerable current density in human subjects (1,2)).

The deduction of a "recovered" barrier versus a "not-yet-recovered" barrier is based upon the confocal visualization of F transport. Compared to skin samples pretreated with iontophoresis, no significant F transport was observed in passive control (control #1) samples. Thus, the F outlining can be considered diagnostic of a perturbed barrier.

Recovery of Post-Iontophoretic Skin Impedance

The recovery of skin impedance was observed following three pretreatments: (1) 0.10 mA/cm^2 applied for 15 minutes; (2) 0.10 mA/cm^2 applied for 2 hrs; and (3) 0.50 mA/cm^2 applied for 2 hrs. Occasional technical difficulties in the latter stages of the experiment meant that the later measurement times were sometimes omitted. When no time was allowed for barrier recovery ($t_{recovery}$ = 0 hrs), impedance values were significantly reduced compared to the pre-iontophoretic hydrated control (see Figure 3, Table I). As a typical example, when a current

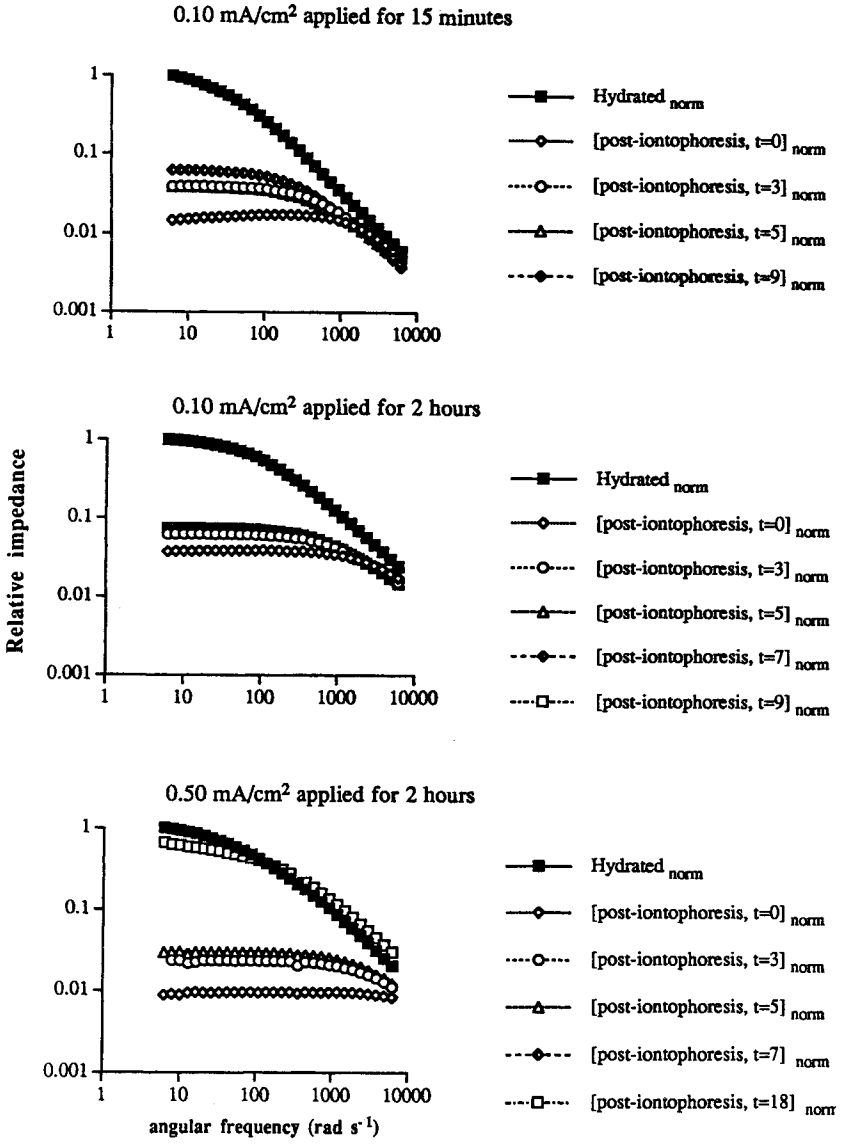

Fig. 3. (Top) Effect of iontophoresis (0.10 mA/cm^2 applied for 15 min) on relative skin impedance at times t = 0, 3, 5, and 9 hrs post-iontophoresis. (Middle) Effect of iontophoresis (0.10 mA/cm^2 applied for 2 hrs) on relative skin impedance at times t = 0, 3, 5, 7 and 9 hrs post-iontophoresis. (Bottom) Effect of iontophoresis (0.50 mA/cm^2 applied for 2 hrs) on relative skin impedance at times t = 0, 3, 5, 7 and 18 hrs post-iontophoresis. The absolute impedance values were normalized with respect to the pre-iontophoretic (hydrated skin) impedance measured at 1 Hz (6.28 rad s^{-1}).

Table I. Relative Impedance Values as a Function of Time Barrier Function Recovery

Time of recovery (hrs)	100 * Relative impedance @ 1 Hz		
	0.1 mA/cm^2—15 min	0.1 mA/cm^2—2 hrs	0.5 mA/cm^2—2 hrs
Hydrated control	100	100	100
0	1.5	3.7	0.9
3	3.9	6.3	2.4
5	3.9	7.2	3.0
7	nd[a]	7.2	2.8
9	6.2	7.4	nd[a]
18	nd[a]	nd[a]	66.3

Note: Relative impedance values (at 1Hz) as a function of time of barrier function recovery measured following iontophoresis across HMS *in vivo* under the following conditions: 0.1 mA/cm^2 for 15 min; 0.1 mA/cm^2 for 2 hrs; and 0.5 mA/cm^2 for 2 hrs.
[a] nd—not determined.

of 0.1 mA/cm^2 was applied for 15 minutes, the relative impedance at 1 Hz dropped from 1.0 (for the hydrated control) to 0.015, a ~67-fold reduction (Table I). This is consistent with similar recent observations (10,12). Three to nine hours post-iontophoresis, HMS impedance had recovered only minimally. Specifically, relative impedance values at 1 Hz were 0.024 to 0.074 (Table 1). Comparison of data obtained from the three iontophoresis regimens (Figure 3), showed no significant difference in the kinetics of skin impedance recovery as the current magnitude and application times were varied. Only in the sample treated with 0.50 mA/cm^2 for 2 hrs were we able to obtain an impedance measurement at the $t_{recovery}$ = 18 hrs time point (Figure 3c). As shown in Table I, the relative impedance at $t_{recovery}$ = 18 hrs was 0.66 at 1 Hz, as compared to only 0.028 after 7 hrs recovery. This extended time frame for recovery is possibly due to the delayed rates in the re-equilibration of ions in the skin. Thus, the time required to restore the skin impedance of hairless mouse to near normal (pre-iontophoretic) levels is longer than 18 hrs. Confocal results indicated that full recovery of the passive permeability barrier required on the order of 24 hours following iontophoresis. It follows that the confocal and impedance measurements are self-consistent.

DISCUSSION

The objectives of the present study were: (1) to characterize, with LSCM and IS, the effect of *in vivo* iontophoresis on the barrier function and electrical properties of HMS, respectively; and (2) to monitor the rates of recovery of these properties to their pretreatment control levels. Other investigators have also shown that skin's passive permeability is increased following application *in vitro* of an iontophoretic current. Wang *et al.* (8) demonstrated that the permeability of HMS to hydrocortisone was increased post-iontophoretically, suggesting a current-induced effect. Kim *et al.* (3) made the same observation for water and mannitol. Inada *et al.* (6) examined the effects of an applied constant *voltage* on human epidermis *in vitro* and assessed the ability of the membrane to recover from the electrical perturbation. The results were interpreted in terms of pore formation leading to increased membrane permeability to mannitol and tetraethylammonium bromide. Recently (5), the flux of acyclovir across nude mouse skin *in vitro* was measured following current pretreatment with phosphate-buffered saline for 4 hours at current densities of 0.25 and 0.50 mA/cm^2. The resulting normalized fluxes were ~2.5-fold higher than passive diffusion. Despite the persuasive nature of the conclusions which may be drawn from the aforementioned work, these investigations (a) do not allow truly relevant recovery information to be obtained (as all experiments were performed *in vitro*, and (b) provide only limited details about the transport pathways (e.g., anatomic location) followed.

The highest applied current density of 0.5 mA/cm^2 used in this study was at the upper limit of clinical acceptability in human subjects (1,2). Consequently, the observed effects of iontophoresis on the passive permeability and impedance properties of HMS represent the extreme end of the normal range. Indeed, 0.1 mA/cm^2 induced less perturbation of the skin barrier compared to iontophoresis at the higher current density. For practical purposes, of course, the current density and duration of current application employed will be the minimum necessary to achieve the desired pharmacological effect with the best effect on the skin.

The LSCM results provide strong evidence that the hair follicle is an important iontophoretic transport pathway and a site at which the skin barrier is altered by current passage. In terms of the kinetics of recovery, LSCM suggests that about 24 hours are necessary for the full restoration of barrier function to pre-iontophoretic levels. The IS data correlated well with this assessment. While IS does not provide *direct* information about iontophoretic transport pathways, it can be used to make mechanistic inferences about iontophoresis (10,16,17). Our experimental post-iontophoretic impedance data are well described by the model. The resistive component of the post-iontophoretic skin impedance (thought to be associated with appendageal pathways) was most affected by current passage (2,11). This conclusion supports mechanistically the LSCM evidence that ion transport during iontophoresis occurs along appendageal pathways (18,19). It should be emphasized, however, that the involvement of other, non-appendageal iontophoretic transport paths cannot be excluded (20) as the nature of such routes, and their importance, are simply not deducible using the experimental tools presently available; in addition, of course, the observations made here using HMS must be confirmed in human skin. A full characterization of mechanism awaits additional, more sophisticated experimental strategies.

ACKNOWLEDGMENTS

Financial support was provided by the U.S. National Institutes of Health (GM15585-03 and HD-27839) and The American Foundation of Pharmaceutical Education Fellowship. We thank Christopher Cullander for confocal expertise.

REFERENCES

1. P. Ledger. *Adv. Drug Del. Rev.* **9**:289–307 (1992).
2. R. R. Burnette and B. Ongpipattanakul. *J. Pharm. Sci.* **77**:132–137 (1988).
3. A. Kim, P. Green, G. Rao, and R. Guy. *Pharm. Res.* **10**:1315–1320 (1993).
4. M. Pikal and S. Shah. *Pharm. Res.* **7**:222–229 (1990).

5. N. Volpato, P. Santi, and P. Colombo. *Pharm. Res.* **12**:1623–1627 (1995).
6. H. Inada, A. Ghanem, and W. Higuchi. *Pharm. Res.* **11**:687–697 (1994).
7. S. M. Sims, W. I. Higuchi, and V. Srinivasan. *Pharm Res.* **9**:1402–9 (1992).
8. Y. Wang, L. V. Allen, L. C. Li, and Y. Tu. *J. Pharm. Sci.* **82**:1140–1144 (1993).
9. R. Brand, P. Singh, E. Aspe-Carranza, H. Maibach, and R. Guy, *Eur. J. Pharm. Biopharm.*, **43**:133–138 (1997).
10. Y. N. Kalia and R. Guy. *Pharm. Res.* **12**:1605–1613 (1995).
11. R. R. Burnette and T. M. Bagniefski. *J. Pharm. Sci.* **77**:492–497 (1988).
12. S. Oh and R. Guy. *Int. J. Pharm.* **124**:137–142 (1995).
13. S. Oh, L. Leung, D. Bommannan, R. Guy, and R. Potts. *J. Control. Rel.* **27**:115–125 (1993).
14. J. DeNuzzio and B. Berner. *J. Control. Rel.* **11**:105–112 (1990).
15. Y. N. Kalia, L. B. Nonato, and R. H. Guy. *Pharm. Res.* **13**:957–960 (1996).
16. K. Kontturi, L. Murtomäki, J. Hirvonen, P. Paronen, and A. Urtti. *Pharm. Res.* **10**:381–385 (1993).
17. K. Kontturi and L. Murtomäki. *Pharm. Res.* **11**:1355–1357 (1994).
18. C. Cullander and R. H. Guy. *Adv. Drug. Del. Rev.* **8**:291–329 (1992).
19. C. Cullander and R. Guy. *Solid State Ionics.* **53–56**:197–206 (1992).
20. N. Monteiro-Riviere, A. Inman, and J. Riviere. *Pharm. Res.* **11**:251–256 (1994).